

## Colloid dynamics and transport of major elements through a boreal river — brackish bay mixing zone

Örjan Gustafsson<sup>a,b,\*</sup>, Anders Widerlund<sup>c</sup>, Per S. Andersson<sup>b</sup>, Johan Ingri<sup>c,d</sup>,  
Per Roos<sup>e</sup>, Anna Ledin<sup>f</sup>

<sup>a</sup> Institute of Applied Environmental Research (ITM), Stockholm University 10691 Stockholm, Sweden

<sup>b</sup> Laboratory for Isotope Geology, Swedish Museum of Natural History, Box 50007, 10405 Stockholm, Sweden

<sup>c</sup> Division of Applied Geology, Luleå University of Technology, 97187 Luleå, Sweden

<sup>d</sup> Department of Geology and Geochemistry, Stockholm University, 10691 Stockholm, Sweden

<sup>e</sup> Department of Radiation Physics, Lund University, 22185 Lund, Sweden

<sup>f</sup> Department of Environmental Science and Engineering, Technical University of Denmark, Bldg. 115, DK-2800 Lyngby, Denmark

Received 6 April 1999; accepted 11 February 2000

### Abstract

A range of biogeochemical methodologies were applied to investigate how aggregation processes affected the phase distribution and mixing of Fe, Si, and organic carbon between the Kalix River and the Bothnic Bay, northernmost Baltic Sea (salinity  $\leq 3$ ; the low-salinity zone (LSZ) was stretching over 60 km in the spring). During the dynamic springflood conditions studied, small  $^{238}\text{U}$ – $^{234}\text{Th}$  disequilibria, low sediment trap fluxes, laboratory mixing experiments, as well as results from an independent two-box, two-dimensional mixing model combine to suggest that no significant removal of Fe, Si, or organic C was occurring in the highly-resolved LSZ. While no conclusions may be drawn based solely on property–salinity plots over narrow salinity ranges, apparently linear graphs for Fe and Si over 3 separate years also suggest minimal removal in this regime. At the same time, size distributions both of elements — from cross-flow ultrafiltration — and of bulk suspended solids — from light scattering (photon correlation spectroscopy [PCS]) — indicated that significant aggregation was taking place.

The aggregation-without-significant-settling scenario in this low-salinity mixing regime, with a geochemistry similar to that of neighboring Russian Arctic rivers, is hypothesized to result from a comparatively high organic-to-detrital matter characteristic of the aggregates. While first principles would indeed suggest that decreasing electrostatic repulsion during mixing lead to aggregation, a low specific density of mineral-poor amorphous organic aggregates may lead to transport of these authigenic particles further away from the river mouth. The role of detrital “sinkers” on vertical removal of suspended organic matter is discussed in the wider context of scavenging mechanisms in the ocean. © 2000 Elsevier Science B.V. All rights reserved.

**Keywords:** Kalix River; Bothnic Bay; Colloids; Low-salinity zone; Aggregation

\* Corresponding author. Laboratory for Isotope Geology, Swedish Museum of Natural History, Box 50007, 10405 Stockholm, Sweden. Tel.: +46-8674-7317; fax: +46-8674-7638.

E-mail address: orjan.gustafsson@itm.su.se (Ö. Gustafsson).

## 1. Introduction

Particle processes taking place in the low-salinity zone (LSZ) are important in estuarine chemistry. It is necessary to elucidate the intricacies of these mechanisms in order to make progress in many diverse questions ranging from predicting the dispersal and fate of coastal contaminants to constructing global mass balances of biogeochemically significant elements. It is well known that the continent-to-ocean transport of several elements may be attenuated by scavenging removal in the estuarine mixing zone. To quantitatively evaluate the key issues of conservative/non-conservative mixing and fluxes of aquatic constituents, one-dimensional, two end-member models have been developed (e.g., Boyle et al., 1974; Officer, 1979); the application of which requires careful attention to the dynamics of end-member compositions (e.g., Loder and Reichard, 1981; Lebo et al., 1994). These widely used theoretical frameworks are based on interpreting the property–salinity plots of the elements of interest, using salinity as a conservative tracer of the mixing between the river and ocean end-members. Such plots frequently suggest that non-conservative behavior may be related to processes occurring in the LSZ (here, defined as salinity  $\leq 3$ ); such indications exist for many different elements and estuarine regimes (e.g., Boyle et al., 1977; Sholkovitz et al., 1978; Elderfield et al., 1990; Shiller and Boyle, 1991; Carroll and Moore, 1994; Dai and Martin, 1995; Kraepiel et al., 1997). Significant tidal mixing — resulting in non-steady state situations and potentially resuspension — in many cases, complicates the discrete sampling of LSZ and limits the effective sampling resolution of this dynamic region.

The objective of this study was to investigate the particle-centric scavenging processes occurring in the LSZ. The Kalix River and its Gulf of Bothnia recipient — a stable salt-wedge highly-stratified type of regime (Pickard and Emery, 1990) — is one of the last major unregulated river systems in Europe. This system offers the advantage over many other LSZs of a minimal tidal circulation (about 1 cm tidal range) and the extended LSZ affords rare spatial resolution, facilitating the detailed study of scavenging processes occurring in the LSZ. After having followed the development of the springflood through

weekly sampling of the lower river (Ingri, 1996; Ingri et al., 2000), we will, in this paper, present results from a process study during peak (snowmelt) runoff conditions, combining a suite of geochemical tools to better understand the dynamics of colloids and larger particles and the relative extents of vertical and horizontal element transport in the LSZ.

What functionally may be considered to constitute a colloidal entity on thermodynamic and hydrodynamic bases has been elaborated upon elsewhere (Gustafsson and Gschwend, 1997). Here, colloids are operationally defined as what is caught between a 0.2- $\mu\text{m}$  and a 3-kD filter. Colloidal and larger Fe/Mn oxides and humic organic matter are believed to be of fundamental importance in the estuarine scavenging of dissolved constituents. Turekian (1977) proposed that studies of the continent–ocean transfer of metals should benefit from applying U–Th radiogenic isotope systematics to trace and time estuarine processes involving major carrier phases. To the best of our knowledge, the present study is the first to combine elemental-based geochemical information on sources, and in colloidal size-fractions, with information on scavenging processes from short-lived  $^{234}\text{Th}$  systematics.

The multi-year field-based observations were complemented by laboratory-based LSZ mixing experiments. Since the interpretation of property–salinity plots over narrow salinity ranges is complicated, acquired insights were also combined into a two-dimensional box model to evaluate the relative importance of horizontal and vertical element transport processes in the LSZ.

## 2. Study site and methods

### 2.1. The Kalix River and its northern Bothnic Bay recipient

The Kalix River, which empties southward into the northernmost Baltic Sea (Fig. 1), is one of the last major unregulated rivers in Europe (mean water discharge, ca.  $300 \text{ m}^3 \text{ s}^{-1}$ ; ca.  $1600 \text{ m}^3 \text{ s}^{-1}$  during spring flood;  $23,600 \text{ km}^2$  drainage area). The Kalix River watershed is situated within the vast boreal zone overlying the northern shields and can thus be considered an easily accessible system that may pro-

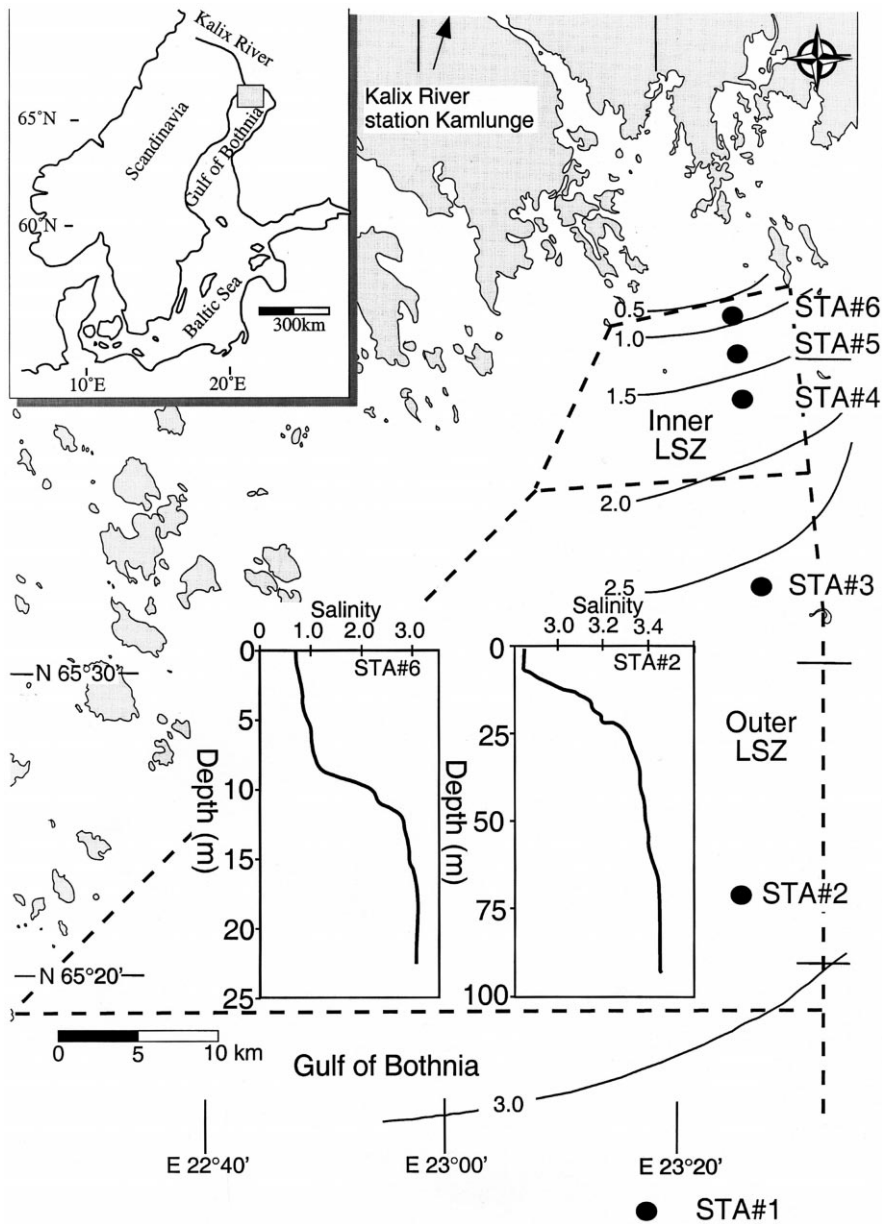


Fig. 1. Map of the Kalix River LSZ. The inset map shows location of the Kalix River in the northernmost Baltic Sea. The sampling stations (marked STA#1 to STA#6 and the Kalix River end-member, station Kamlunge) are seen to cover a 60-km stretch of the 0–3 salinity range of the LSZ. Isohaline lines for the mixed surface water indicates the spreading of the fresh water plume. Conductivity–temperature–depth (CTD) profiles from stations 2 and 6 (Table 1) demonstrate the existence of a surface mixed layer depth.

vide a representative picture of the many large Siberian “black rivers” draining northward into the Arctic Ocean (Romankevich, 1984; Dai and Martin, 1995).

Furthermore, the studied regime is an ideal location for studying fundamental processes in the LSZ as it exhibits extremely weak tidal pumping ( $< 1 \text{ cm s}^{-1}$ ) and has no significant secondary tributaries

complicating its mixing with the northern reaches of the Bothnic Bay. This facilitates good salinity resolution of the elsewhere hard-to-sample, dynamic portion of an estuary (the LSZ region stretches here over 60 km in the spring).

Adding to its suitability as a model LSZ, there is plenty of useful background information available on the hydrology, geology, and geochemistry of the Kalix River drainage basin and its Gulf of Bothnia recipient (e.g., Boström et al., 1982; Ingri and Pontér, 1986; Pontér et al., 1990, 1992; Ingri and Widerlund, 1994; Andersson et al., 1995, 1998; Ingri, 1996; Öhlander et al., 1996; Widerlund, 1996; Ingri et al., 1997, 2000; Porcelli et al., 1997). These studies combine to produce a picture of a system with large seasonal variations, including effects from ice-coverage during December–May. A large fraction of the river suspended phase consists of autochthonous Fe and Mn oxyhydroxides (Pontér et al., 1990, 1992; Ingri and Widerlund, 1994; Ingri, 1996). These appear to act as carriers of, for instance, alkali and alkaline-earth elements (Ingri and Widerlund, 1994) as well as in significant ways affect the land–ocean transfer of several U and Th isotopes (Andersson et al., 1995, 1998; Porcelli et al., 1997). While these previous results suggest the importance of oxide and organic colloidal species, the importance of non-conservative mixing in the LSZ is being debated (Widerlund, 1996; Porcelli et al., 1997). To add to these recent element/isotope-centric investigations, the current study seeks to elucidate the intrinsic particle processes affecting the behavior of major elements during mixing at low salinities. We stress that the studied regime is the 0–3 low salinity mixing zone of Kalix River and the Bothnic Bay, and not mixing with the salinity  $\approx 35$  North Sea end-member. The Bothnic Bay is topographically and bathymetrically constrained and its mixing with the rest of the Baltic Sea is thus sluggish and limited. The Baltic Sea is better described as a fjord than as an estuary. It has six distinct bays/gulfs, and some 250 major tributaries with several geochemically different draining regimes.

## 2.2. Sampling strategy

Sampling of the low-salinity mixing zone was implemented during height of springflood discharge

(late May–early June). Timing of the field efforts in 1991, 1992, and 1997 were afforded through both historic (e.g., Ingri, 1996; Widerlund, 1996), and in 1997 immediately preceding, monitoring of the river hydrology and geochemistry with weekly intervals at the lower river station Kamlunge (Ingri et al., 2000). There is a significant variability of the freshwater end-member in hydraulic discharge and geochemical composition during this period of the year (Ingri, 1996; Ingri et al., 2000).

On the 1997 expedition, the LSZ was first characterized spatially by performing CTD (conductivity–temperature–depth) mapping in a zigzag pattern throughout the estuary. Then, six sampling stations covering the 0.6–3 salinity range were occupied and biogeochemically detailed using a wide range of analytical approaches. In addition, cylindrical sediment traps with an aspect ratio (height to width) of 5 (Larsson et al., 1986) were deployed right below the pycnocline at stations 2, 4, and 6 (Fig. 1) during the cruise and recovered 3 weeks later.

### 2.2.1. Size fractionation

The on-line fractionation of trace and major elements into operationally-defined dissolved ( $< 3$  kD), colloidal (3 kD–0.2  $\mu\text{m}$ ), and larger particulate ( $> 0.2$   $\mu\text{m}$ ) pools was, in 1997, afforded by development of a shipboard sequential cross-flow filtration (CFF) system. During the calm-weather conditions of the cruise, the surface water intake line was extended 30 m away from the ship's upwind side with an extendable crane. Water from the center of the mixed surface layer ( $z_{\text{mix}}$  ranged from 4 to 8 m; Table 1 and Fig. 1) was peristaltically pumped (Masterflex, Millipore) through 0.5 M HCl acid-leached polyimide and silicon tubing onboard and directly processed (Dominador Pumps, Dominador) through two CFF systems (Pellicon, Millipore) arranged in series and plumbed with 0.5 M HCl acid-washed polypropylene tubing. The CFF system is described in greater detail in Ingri et al. (2000). Immediately preceding each new sampling, both the 0.2- $\mu\text{m}$  PVDF (0.46- $\text{m}^2$  filter area) and the 3-kD regenerated cellulose ( $2 \times 0.46$   $\text{m}^2$  filter area) CFF membranes were subjected to acid- (0.5 M HCl) and base- (0.1 M NaOH) leach cleaning protocol and water preconditioning. Also following protocols developed earlier (Gustafsson et al., 1996), the in-

Table 1  
Surface water characteristics for the Kalix River–Bothnic Bay mixing zone during spring runoff conditions 1997

	Station 6	Station 5	Station 4	Station 3	Station 2	Station 1
Distance from river mouth (km)	1	2	6	17	35	65
Mixed layer depth (m)	8	5	6	4	5	5
Conductivity (mS/cm)	2.15	2.83	3.40	4.63	4.91	5.15
Salinity <sup>a</sup>	“1.40”	“1.62”	“1.92”	2.69	2.87	3.03
pH	7.38	7.33	7.52	7.63	7.78	7.97
Alkalinity (mM HCO <sub>3</sub> equiv.)	0.524	0.441	0.484	0.701	0.681	0.830
Primary production (μM C day <sup>-1</sup> )	0.07	0.01	1.10	0.22	1.48	0.54
Bacterial production (10 <sup>8</sup> cell/1 day <sup>-1</sup> )	6.6	4.8	5.9	1.9	9.3	2.3
HPO <sub>4</sub> <sup>2-</sup> (μg/1 P)	2.1	2.8	1.6	1.5	0.8	1.1
NO <sub>3</sub> <sup>-</sup> (μg/1 N)	50.8	62.8	75.6	91.9	94.8	77.8
H <sub>2</sub> SiO <sub>3</sub> (μg/1 Si)	1850	1790	1710	1240	1130	1010
Humic substances [HS] (μg/1 QSE)	47.7	43.0	32.7	22.7	18.9	14.5
SPM (mg/l)	2.09	2.38	1.87	1.47	1.47	1.40
TOC (μM)	505	439	405	344	324	306
POC (μM)	18.3	23.8	25.2	13.2	19.2	20.2
COC (μM)	80	58	52	82	n/a	103
DOC (μM)	330	350	340	420	260	190
δ <sup>13</sup> C–POC <sup>b</sup> (per mil PDB)	–30.9	–30.3	–30.3	–29.8	–29.8	–28.9

<sup>a</sup>Since the Practical Salinity Scale is only defined down to salinity 2, all values below 2 are regarded as “unofficial”, but included here to define extent of mixing.

<sup>b</sup>The mean relative standard deviation of these measurements (six samples each measured in triplicates) was 0.6%.

tegrity and actual cut-off of the 3-kD membrane was evaluated using a set of colloid standards. Tests of the CFF system suggest that the cut-off indeed was in the vicinity of 3 kD and that it was possible to achieve minimal losses of carbohydrate and humic-like colloid standards when operated under realistic field conditions (Gustafsson and Ingri, in prep.). Further, the light scattering measurements (see below) showed that the colloids passing through the filter with 0.2 μm cut-off indeed had sizes below this. Corresponding measurements on the water samples passing through the 3-kD CFF gave no detectable signal.

The 3-kD CFFs were operated under a 0.8–1.0 bar transmembrane pressure, yielding a permeate (i.e., < 3 kD filtrate) flow rate of 300–400 ml/min and retentate (i.e., recirculating > 3 kD crossflow) flow rate of 3–4 l/min. The final concentration factor ( $c_f = V_{\text{permeate}}/V_{\text{retentate}} + 1$ ) for the 0.2-μm system was 12–30 and sampling with the smaller 3-kD filter was halted at  $c_f = 11$ –22. The permeate was subsampled on-line at evenly-spaced intervals to avoid any significant effects of retentate breakthrough at near-final  $c_f$  (Buessler et al., 1996; Dai et al., 1998).

The obtained retentate reservoir was subsequently split for different analyses. For inorganic major and trace element analyses, the retentate samples were collected on acid-leached (0.9 M acetic acid) 0.2-μm membrane filters (GSWP, Millipore) by means of vacuum filtration in a shipboard HEPA-filtered laminar flow bench employing trace-clean protocols.

Samples for total, colloidal, and dissolved organic carbon (TOC = total, unfiltered; COC = CFF-isolated colloidal pool 3 kD–0.2 μm; DOC ≤ 3-kD ultrafiltered “truly dissolved” permeate) were collected in pre-combusted amber glass bottles with Al-foil-covered, Teflon-lined caps and immediately stored cold. Samples for particulate organic carbon (POC) and stable C and N isotopes were filtered onto pre-combusted glass fiber filters (GF/F, Whatman) using a stainless steel filter holder.

#### 2.2.2. Collection of <sup>234</sup>Th

High-volume sampling (1000–2000 l) for short-lived <sup>234</sup>Th was afforded by in-situ pumping from the middle of the mixed surface layer to a deckboard filtration and extraction unit. After removing oversized particles using a 100-μm nylon screen, the water was passed through a 0.2-μm polypropylene

filter cartridge (Osmonics) and two serially coupled MnO<sub>2</sub>-impregnated adsorbents (prepared according to Hartman and Buesseler, 1994).

Samples for quantification of unfiltered (total) activities of <sup>234</sup>Th was collected by the same in-situ pump into a 200-l plastic drum. A known amount (in the range 40–50 mBq) <sup>230</sup>Th yield tracer was added to this stirred reservoir. After tracer equilibration (1 h), a magnesium oxide precipitate, quantitatively known to scavenge Th, was induced by addition of magnesium chloride salt and sodium hydroxide. This was allowed to settle and collected for further processing at shore-based facilities. <sup>238</sup>U was subsampled online into acid-leached polyethylene bottles.

### 2.2.3. Sampling of ancillary parameters

Sampling and analysis of ancillary parameters such as nutrients, alkalinity, pH, total suspended matter (TSM), CTD parameters, as well as primary (<sup>14</sup>C-carbonate incubation) and bacterial production (<sup>3</sup>H-leucine incubation) were performed using standard marine chemistry protocols at Umeå Marine Research Center (e.g., HELCOM, 1988).

### 2.3. Laboratory mixing experiments

Mixing experiments were performed using Kalix River water and Bothnic Bay surface water collected in October 1995. The mixing experiments (methodology after Sholkovitz, 1976) were commenced within 24 h of sample collection. Aliquots of 0.45 µm membrane (HAWP cellulose nitrate; Millipore) filtered river and Bothnic Bay (salinity 2.7) brackish water were mixed in varying proportions (total volume 750 ml) in acid-leached polyethylene bottles. The solutions were mixed by hand for 1–2 min, equilibrated for 24 h in the dark at room temperature and again filtered through 0.45-µm using a syringe.

### 2.4. Analyses

#### 2.4.1. Major inorganic elements

Quantification of iron and silica in the dissolved, colloidal, and particulate samples were done with inductively-coupled plasma (ICP) instruments, normally with atomic emission spectroscopy (ICP-AES), but for Fe in 1997 with high-resolution mass spectrometry (HR-ICP-MS) detection in co-operation with

SGAB Analys (Luleå, Sweden). The analytical uncertainties for these methods (expressed as  $\pm 1$  S.D. for  $n = 3–4$ ) were, in 1991 and 1992, on ICP-AES  $\pm 10\%$  for Fe and  $\pm 1\%$  for Si (also 1997 Si data), while it was only  $\pm 2\%$  for Fe in 1997 on HR-ICP-MS (Rodushkin and Ruth, 1997). The analysis of colloidal retentate samples were performed with preceding microwave digestion (Ingri et al., 2000). Particulate ( $> 0.2$  µm) retentate samples collected on 0.2-µm membrane filters were subjected to metaborate digestion treatment (Burman et al., 1978; Ödman et al., 1999) before ICP-AES/MS quantification.

#### 2.4.2. Organic carbon (OC) components

POC and the stable carbon isotope composition of POC was determined with an elemental analyzer (Perkin Elmer CHN 2400) coupled to a Micromass Optima isotope ratio monitoring mass spectrometer (irm-MS) and reported relative to the PeeDee belemnite standard. Samples for total, colloidal and DOC was, after acidification and purging of inorganic carbon, determined with high-temperature catalytic oxidation methods. TOC was quantified in triplicates using a Shimadzu TOC-5000, while the size-fractionated COC and DOC were analyzed in duplicates with an Ionics 555. A Milli-Q blank on the order of 10 µM was, in both cases, subtracted from the obtained data. The six TOC analyses of this study had a relative standard deviation (R.S.D.) of  $2.1 \pm 1.3\%$  (1 S.D.) and the DOC/COC data showed a  $< 3\%$  R.S.D. ( $n \approx 30$ ). It was not possible to collect TOC and COC/DOC samples integrated over the same time period due to the long sampling time of the CFF. Hence, it is unfortunately not possible to expect a 100% mass balance agreement between the TOC and the COC plus DOC.

Humic substance (HS) abundance (unfiltered) was determined fluorometrically in triplicates (LS 30; Perkin Elmer) using the excitation/emission wavelength pair 350/450 nm, which have previously been shown to be appropriate for the chromophoric moieties of HS in the northern Baltic Sea (Kalle, 1949; Skoog et al., 1996). The conditions under which the instrument was operated was calibrated using quinine sulfate, and the fluorescence intensities obtained for the natural water samples are thus reported as quinine sulfate equivalents (µg/l QSE).

#### 2.4.3. Solid matter size distribution by PCS

Samples for characterization of the suspended solid matter by light scattering (LS), for estimation of relative concentrations, and PCS, for size distribution measurements, were subsampled shipboard into Milli-Q pre-washed plastic bottles both before any filtration (i.e., “total phase”) and from the CFF fractions. These samples were immediately transported by speed-boat to the shore-based PCS facility at Luleå University of Technology for further processing and analyses. The samples were stored in the dark and at the sampling temperature during this transport. All measurements were made within 12 h of original sampling.

Relative concentrations and size distributions of the particulate matter were analyzed by LS and PCS employing a Brookhaven Instruments BI-200-SM laser light scattering system equipped with a BI-9000 autocorrelator and a 2-W argon laser (the latter from Lexel). The instrument was operated at a wavelength of 514 nm and a scattering angle of 90°. The aperture was varied in the range 100–400 while the laser power was varied in the range 50–1000 mW to receive an output in light intensity in the range 50–500 kcps (counts per second) under varying colloid concentrations.

The auto-correlation function, for size distribution estimates, was in the present study solved by inverse Laplace transform routines by the original instrument software (NNLS). The general theory of PCS has been presented elsewhere (e.g., Chu, 1974; Berne and Pecora, 1976; Schurtenberger and Newman, 1993).

The main limitation with PCS is the risk for underestimation of small particles compared to larger ones due to the greater scattering intensities of larger particles. It has, therefore, been suggested that the measurements of natural colloidal matter should be performed at different scattering angles and/or to use some fractionation step (sedimentation, centrifugation, filtration) to exclude the coarse material prior to the measurements (Ledin et al., 1993; Perret et al., 1994). In the present study, the samples were measured after sedimentation for approximately 1 h and both preceding as well as immediately after filtration through polycarbonate membranes (pore sizes of 0.80 and 0.20  $\mu\text{m}$ , respectively). Great care was taken to maintain the original diameters of the pores, by

selecting individual maximum filtration volumes for each sample, in order to avoid clogging of the filters (Karlsson et al., 1994). The three different data sets received for each water sample with this procedure, were carefully consolidated during the evaluation of the results. The impact of different scattering angles on the obtained size distribution will be presented elsewhere in a separate part of this study (Schoeman et al., in prep).

#### 2.4.4. Scanning electron microscopy (SEM)

Filters for SEM characterization of individual suspended particles were covered with carbon and examined with a Cam Scan s 480-DV SEM coupled with a Link eXL energy-dispersive X-ray spectrometer (EDS). For the quantitative analysis, a Co standard was used.

#### 2.4.5. $^{234}\text{Th}$ and $^{238}\text{U}$ isotopes

The short-lived isotope  $^{234}\text{Th}$  ( $t_{1/2} = 24$  days) present at low abundance ( $< 0.3$  dpm/l) in these low-salinity samples were radiochemically purified and quantified by low-level beta counting techniques largely following previously published protocols (e.g., Buesseler et al., 1992b; Gustafsson et al., 1998). Briefly, following the combustion of cartridges at 500°C for 12 h in ceramic holders, the residue was brought up in aqua regia and  $^{229}\text{Th}$  (in the range 20–30 mBq) was added as a yield tracer. Two ion exchange (Dowex AG1-X8) columns were used. The first was eluted with 9M HCl to separate U and Th, and the second with 8 M  $\text{HNO}_3$  in order to remove remaining beta emitting impurities (Buesseler et al., 1992b). For some  $\text{MnO}_2$ -adsorbed samples, an initial tri-*n*-butyl phosphate extraction of U and Th from 6 M  $\text{HNO}_3$  was performed in order to remove bulk material and thus prevent clogging of the anion exchange columns. Thorium and uranium was sequentially back-extracted from the organic phase with 1.5 M HCl and water, respectively, after diluting the TBP with xylol.

The purified Th fractions were electroplated onto stainless steel planchets. The quantification of  $^{229}\text{Th}$  and  $^{230}\text{Th}$  yield tracers were performed using  $\alpha$ -spectrometry. The surface barrier or PIPS detectors (efficiencies of detectors ranged from 0.227 to 0.348) are regularly calibrated using certified alpha sources. In calculating the tracer recoveries, both the detector

background surrounding the peak of the Th isotope, as well as the natural abundance (for  $^{230}\text{Th}$ , estimated from the  $^{232}\text{Th}$  abundance and  $^{230}\text{Th}/^{232}\text{Th}$  ratios obtained from  $\text{MnO}_2$  adsorbents where  $^{229}\text{Th}$  tracer was used). Th recoveries through the entire procedure were for unfiltered precipitations  $0.65 \pm 0.19$  ( $n = 10$ ; range 0.3–0.95;  $^{230}\text{Th}$  tracer) and for  $\text{MnO}_2$  and filter cartridges  $0.85 \pm 0.16$  ( $n = 22$ ; range 0.5–1;  $^{229}\text{Th}$  tracer). Stainless steel planchets were wrapped in 12 mg/cm<sup>2</sup> thick Al foil as absorption filter to block non-desired and potentially interfering beta emitters (primarily  $^{212}\text{Bi}$  and  $^{212}\text{Pb}$ ). Low-level beta-counting (efficiency calibrated using  $^{238}\text{U}$  sources in equilibrium with  $^{234}\text{Th}$ ) of the stronger emitting  $^{234}\text{Th}$  product  $^{234}\text{Pa}$  was performed for  $10 \times 200$  min and repeated with approximately a weekly interval over 1–2 half-lives. Additionally, significant beta activity from  $^{228}\text{Th}$  decay products in samples from this runoff area was accounted for by quantifying  $^{228}\text{Th}$  activity also with alpha spectrometry and subtracting the resulting contribution to the total beta signal (about 10%, Roos et al., in prep.).

$^{234}\text{Th}$  activities — corrected for background signals, method recovery, and U ingrowth — were decay-corrected to the mid-point of sample collection. Errors (1.2–5.2% at the 95% confidence limit) were constrained by the goodness of the fit of the raw counts to the  $^{234}\text{Th}$  decay curves.

The  $^{238}\text{U}$  in these brackish waters was determined using isotope dilution on a Finnigan MAT 261 Thermal Ionization Mass Spectrometer (TIMS) following procedures in Chen et al. (1986) and Andersson et al. (1998).

### 3. Results and discussion

#### 3.1. Characteristics and behavior of iron and silica

##### 3.1.1. Mixing zone transects

While conservativeness is difficult to evaluate in the dynamic LSZ, a suite of geochemical tools combine to suggest that there exists no evidence for scavenging removal of either Fe or Si from the Kalix–Bothnic LSZ. Fe decreased in an apparently conservative manner from 4 to 6  $\mu\text{M}$  at the river mouth (salinity about 0.5) to about 1  $\mu\text{M}$  at salinity 3 (Fig. 2a). Si dropped linearly through the same

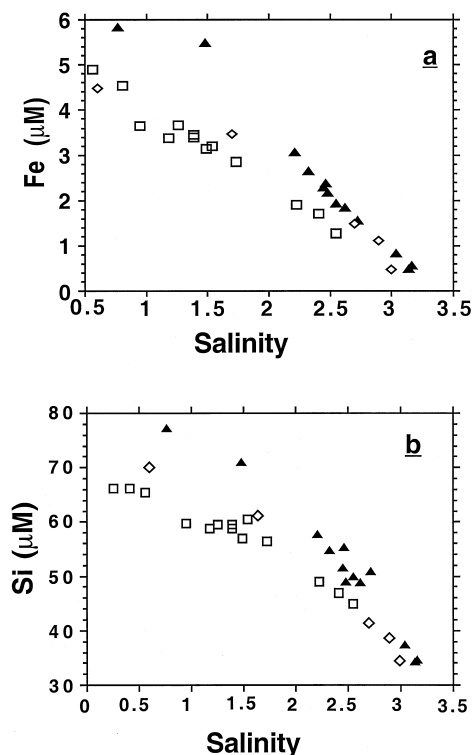


Fig. 2. LSZ mixing behavior of filtered Fe (a) and Si (b) in the Kalix LSZ during springflood in 3 different years: June 1991 (open squares:  $< 0.45 \mu\text{M}$ ); June 1992 (filled triangles:  $< 0.45 \mu\text{M}$ ); June 1997 (open diamonds:  $< 0.2 \mu\text{M}$ ).

LSZ from 70–80 to 35  $\mu\text{M}$  (Fig. 2b). The property–salinity plots of Fe and Si, representing the supposedly important  $< 3$  salinity region, during discharge season in 3 different years, suggest an apparently linear mixing behavior albeit we stress that no firm conclusions may be drawn to this respect based solely on such plots in a dynamic LSZ. However, if one were to fit those plots with a linear equation one would find that dilution explains over 90% of the data in all six cases. It must be emphasized that these LSZ plots should not be extrapolated beyond the salinity 3 limit of the open Bothnic Sea. The exchange between this northernmost Bay of the Baltic Sea with the waters to the south is highly restricted. Furthermore, a multitude of other rivers with different geochemistry than the Kalix River are emptying into the southward-flowing western return flow obscuring any possibilities to reasonable extend any linear mixing of the studied LSZ with higher

saline waters in the direction of the North Sea. It should also be emphasized that even interpreting property–salinity trends in the 0–3 salinity region is complicated due to the narrow salinity range as well as the non-steady state of the river end-member composition (Ingri, 1996; Ingri et al., 2000). Hence, we are drawing no conclusions regarding conservativeness during LSZ mixing based solely on such plots.

Cross-flow ultrafiltration revealed that the majority of the Fe  $< 0.2 \mu\text{m}$  was in the colloidal form (Table 2) throughout the transect. Some losses of Fe to the CFF system were apparent as the recovery ( $R\% = (\text{dissolved} + \text{colloidal})/\text{feed}$ ) around the 3-kD membrane was decreasing from 83% at innermost station to 53% at offshoremost station 1 (mean  $R\% = 67 \pm 9\%$ ; 1 S.D.). Correspondingly, the  $R\%$  for Si was 100–115% (mean  $R\% = 105 \pm 6\%$ ). However, since information on colloidal abundances is of great benefit when assessing the particle dynamics during mixing, the present data — even when taking the losses into explicit account — provides useful upper and lower limits of the importance of colloidal forms. The isolated colloidal pool — representing a minimum of Fe colloids — was contrasted to both the total Fe concentration fed into the CFF and to the sum of the CFF-isolated dissolved and colloidal concentrations (Table 2). These

CFF Fe data demonstrates that of the filter-passing (i.e.,  $< 0.2 \mu\text{m}$ ) fraction the majority of the Fe is colloidal, ranging from 75% to 90% at station 6 off the river mouth to 44–84% at the outermost station 1. In contrast, the fraction of  $< 0.2\text{-}\mu\text{m}$  Si that exists in a colloidal form is less than 1% throughout the entire transect (Table 2).

### 3.1.2. Laboratory mixing experiments

Although the simple batch mixing procedure employed here may not include all processes taking place in a natural estuary (e.g., coagulation induced by shear, bottom impaction and resuspension), such experiments offer the advantage of constant end-member compositions and have provided important insights into the mechanisms of estuarine mixing (e.g., Sholkovitz, 1976; Boyle et al., 1977; Sholkovitz et al., 1978). The mixing experiments of  $0.45\text{-}\mu\text{m}$  pre-filtered Fe (Fig. 3a) and Si (Fig. 3b) suggested that little or no flocculation was taking place early during estuarine mixing. This is consistent with the corresponding field-based mixing of these elements (Fig. 2). It is well known that salinity influences the kinetics of coagulation (e.g., Boyle et al., 1977). It is probable that the lack of removal in the LSZ is reflecting slow kinetics and that removal commences at salinities above 3; which lies beyond the scope of

Table 2

Cross-flow ultrafiltration results on the phase distribution of Fe and Si in the Kalix–Bothnic Bay LSZ during spring runoff conditions

	River <sup>a</sup>	Station 6	Station 5	Station 4	Station 3	Station 2	Station 1
Distance from river mouth (km)	–5	1	2	6	17	35	65
<i>Fe</i> ( $\mu\text{M}$ )							
$< 0.2 \mu\text{m}$ Filtrate	2.15	0.44	0.41	0.50	0.31	0.23	0.23
3 kD– $0.2 \mu\text{m}$ Colloids	1.6	0.32	0.21	0.30	0.16	0.13	0.10
$< 3$ kD Dissolved	0.070	0.038	0.036	0.018	0.030	0.018	0.020
CFF recovery ( $R\%$ )	76%	83%	64%	65%	63%	62%	53%
Colloids/filtrate	0.72	0.75	0.55	0.61	0.53	0.54	0.44
Colloids/(dissolved + colloids)	0.96	0.90	0.86	0.94	0.84	0.87	0.84
<i>Si</i> ( $\mu\text{M}$ )							
$< 0.2 \mu\text{m}$ Filtrate	84.7	59.1	55.2	52.3	36.3	33.8	30.6
3 kD– $0.2 \mu\text{m}$ Colloids	0.17	0.28	0.20	0.15	0.25	0.29	0.086
$< 3$ kD Dissolved	93.9	59.1	55.2	53.4	38.1	34.9	34.9
CFF recovery ( $R\%$ )	110%	100%	100%	102%	106%	104%	115%
Colloids/filtrate	0.002	0.005	0.004	0.003	0.007	0.009	0.003
Colloids/(dissolved + colloids)	0.002	0.005	0.004	0.003	0.006	0.008	0.002

<sup>a</sup>River station Kamlunge sampled 29 May, 1997.

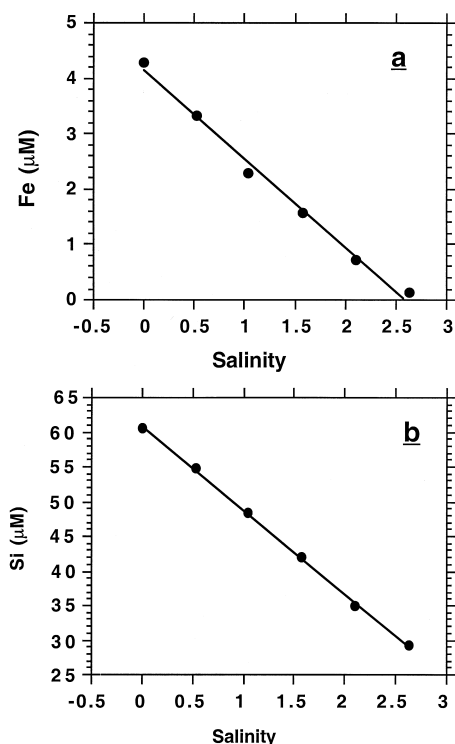


Fig. 3. Property–salinity plots of 24-h laboratory mixing experiments of filtered ( $< 0.45 \mu\text{m}$ ) Fe (a) and Si (b). Lines indicate the theoretical conservative mixing behavior between Kalix River and Bothnic Bay end-member waters collected in October 1995.

the present study. We note that Boyle et al. (1977) truncated their mixing experiments after 30 min, while the experiments in this study were allowed to equilibrate for 24 h — a more relevant time scale for mixing through the Kalix LSZ — before we concluded that insignificant removal had taken place.

While Si is known to mix conservatively (e.g., Boyle et al. 1974), the apparently conservative LSZ behavior for Fe deduced from Fe–salinity plots in both several field years (Fig. 2a) and in laboratory mixing experiments (Fig. 3) contrasts with what has become expected from previous mixing studies of this element in low salinity regimes (e.g., Boyle et al., 1977; Sholkovitz et al., 1978; Dai and Martin, 1995). Why is Fe apparently not removed in the LSZ of the Kalix and plausibly neither from many other similar systems? This question is addressed below using a suite of simultaneously obtained biogeochemical data.

### 3.2. Characteristics and behavior of the organic and particulate matter

While it is not possible to draw any firm conclusions regarding (non-)conservativeness based on property–salinity plots covering narrow salinity ranges for any element, as for Fe and Si, there are no indications of non-conservative mixing for TOC nor for HS as a function of LSZ conductivity (Table 1).

The Kalix River and its LSZ is rich in organic matter during springflood (600–800  $\mu\text{M}$  in the lower river; Ingri, 1996; Ingri et al., 2000). In fact, despite the significantly increased hydraulic discharge during this period, the total organic carbon concentrations in northern Baltic rivers have been shown to reach their yearly maxima at this time (Heikkinen, 1994; Ingri, 1996). The TOC decreased from above 500  $\mu\text{M}$  at our innermost station to near 300  $\mu\text{M}$  at salinity 3.0 (65 km off the river mouth) at the outer reaches of the estuarine LSZ (Table 1). These TOC levels agreed with previous reports, as did the HS data, for this region and season (Wedborg et al., 1994; Petterson et al., 1997). POC was 4–7% of TOC and 11–17% of TSM which is in the same range as ratios found previously in the Kalix LSZ (Widerlund, 1996).

The TOC/Fe ratio is high in the Kalix during springflood (about 100 on a mole basis). In comparison, the Amazon river value is a factor of 5–10 lower (Sholkovitz et al., 1978). Further, the Fe/Ti ratios in the  $> 0.2\text{-}\mu\text{m}$  suspended particles were elevated by about a factor of 8 (mole ratio; data not shown) relative to average crust and local till, indicating a largely non-detrital form of Fe. In support of Fe existing in this system as primarily autochthonous iron oxyhydroxides and not as high-density Fe-rich detrital particles is the S.E.M./EDS microscopy results ( $76 \pm 0.9\%$  Fe; Fig. 4). Taken together, this suggests that the reason for Fe not settling in this LSZ may be either that it is associated with abundant humic matter or that it is merely forming loosely aggregated oxyhydroxide flocs, or a combination thereof. However, this hypothesis raises a second question: why is the humic material not scavenged in the Kalix LSZ? Or is it?

At the same time as both TOC and HS were decreasing, the POC/TOC ratio was increasing (Table 1). One might expect the reverse as coagulation

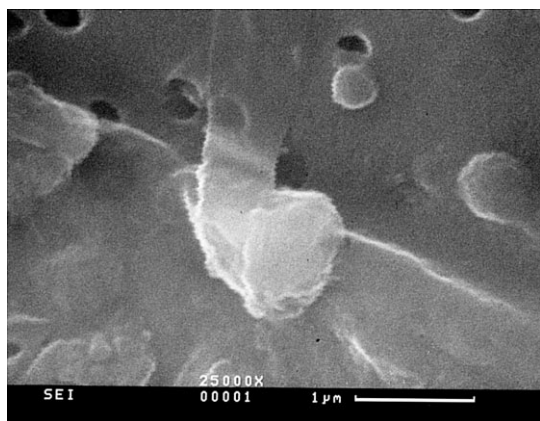


Fig. 4. A typical scanning electron micrograph of suspended Fe-rich particle (center of figure) from the surface water of the Kalix River LSZ (this photomicrograph is from June 1992). The scale bar is 1  $\mu\text{m}$ . S.E.M./EDS analysis of this particle showed that its chemical composition was  $79.0 \pm 0.9$  wt.% Fe (1 S.D.), thus strongly suggesting that this spherical particle is an autochthonous iron oxyhydroxide.

theory holds that with decreasing overall suspended load, there will be a smaller fraction in the larger size bins since a lower collision frequency would yield increased importance of settling over coagulation (e.g., Farley and Morel, 1986; Gustafsson and Gschwend, 1997). However, this assumes a constant  $\alpha$  (sticking coefficient); increasing ionic strength offshore is likely to lead to decreasing electrostatic repulsion and thus a larger fraction of the collisions resulting in aggregation (i.e.,  $\alpha$  proportional to conductivity in the LSZ). The increasing POC/TOC ratio may be related to the simultaneously decreasing HS/TOC. Trends of diminishing HS/TOC (Table 1) can plausibly be explained by preferential settling of HS, decrease in the actual number of fluorophores per gram HS (Wedborg et al., 1994), or photodegradation/photobleaching (Skoog et al., 1996).

However, it may equally well be a result of enhanced aggregation of humic matter onto/into larger size fractions as charge shielding increases with salinity. As the humic macromolecules coalesce into larger entities, the exposed surface area to volume ratio will decrease. As has been elaborated upon elsewhere, one may anticipate that the hydrophobic fluorophore moieties may form the center core in a tertiary structure of such larger aggregates (Kershaw, 1986; Gustafsson and Gschwend, 1997). Hence, it is

reasonable to expect that as a result of humic matter aggregation, less fluorescence per mole of fluorophore structure may be seen, either due to “shading” in the interior of the aggregate, or because of rapid radiationless quenching (Lakowicz, 1983). The implication of such a dynamically varying fluorescence quantum yield of humic moieties for fate studies of HS in estuaries is that spectrofluorometric quantification of HS may not accurately reflect variations in humic matter concentrations. Wedborg et al. (1994) calibrated the spectrofluorometric HS measurements with actual quantification of the humic matter mass concentration on four separate occasions at the same location as our outermost station. Taking typical river HS as 52% C (Thurman, 1985), we calculated from the results of Wedborg et al. (1994) a calibration/conversion factor (i.e., reflecting a bulk humic fluorescence quantum yield) of 400  $\mu\text{g/l C}$  per  $\mu\text{g/l QSE}$  for humic matter at this northern Bothnic Bay location. Thus, converting our HS data from QSE basis to the humic carbon mass scale would suggest that the HS represent 85–100% of the TOC at our two outermost LSZ stations. However, applying this same calibration factor throughout the LSZ would hold that at the innermost three stations the fraction of the TOC that exists as humic matter would be an impossible 140–180%. This suggests a lower fluorescence quantum yield at higher salinities, presumably due to a closer “packaging” of the aggregates. Taken together, there are good reasons to believe that humic matter constitutes a dominant portion of the TOC throughout the transect but that its fluorescence may be partially quenched as it is aggregating in its transfer through the LSZ of estuaries such as that off the Kalix River.

A scenario of transectual aggregation (without significant settling) is further corroborated by stable carbon isotopes, size-fractionated organic carbon and PCS data. Stable isotope analysis of POC ( $\delta^{13}\text{C}$  values relative to PDB standard) showed only small variations between the six LSZ stations ( $\delta^{13}\text{C} = -29$  to  $-31$  per mil; Table 1); values were strongly suggestive of an overwhelming contribution of terrestrial vascular plant material, which could be HS. A dominating land-derived source of the estuarine organic matter is supported by the low primary production rates ( $0.01\text{--}1 \mu\text{M C day}^{-1}$ ; Table 1), which are at the low end of what has been reported

as an annual average for the northern Baltic Sea (Elmgren, 1984). Hence, we conclude that increasing POC/TOC throughout the transect is most likely due to abiotic aggregation as opposed to reflecting primary production. An aggregation process is also consistent with the finding of highest COC/DOC ratio at the outermost station (Table 1).

The light scattering data suggest an increase in the mean colloid diameter in the offshore direction (Fig. 5). For example, the average dimension increased from approximately 325 to around 600 nm in going from station 4 to station 2. However, it should also be pointed out that the data became more scattered outside of station 4, indicating the presence of larger particles known to cause the observed problem for the instrument to resolve the autocorrelation function. The particulate size distribution within each sample, as revealed by PCS, could be divided in two different groups. The first group/regime dominating at the river end-member and the innermost estuary stations contained colloids with diameters in the two ranges: 40–120 and 200–400 nm (Fig. 6a). The other group, typical for the outer stations, also exhibited a bimodal distribution. However, here the coarser mode were generally broader; 200–600 nm, and sometimes up to 1000 nm (Fig. 6b). These PCS findings lend further support to colloids remaining in

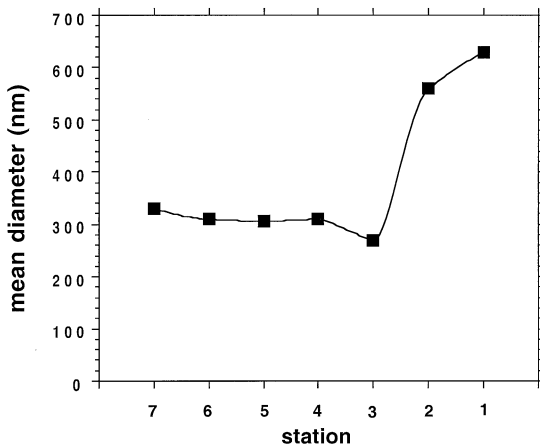


Fig. 5. Mean suspended particle diameter at the stations of the Kalix LSZ in June 1997 deduced from light scattering techniques (PCS). Increase in mean scattering size at the two outermost stations may reflect aggregation as suggested by, for instance, the filter-based size distributions of organic carbon throughout the transect.

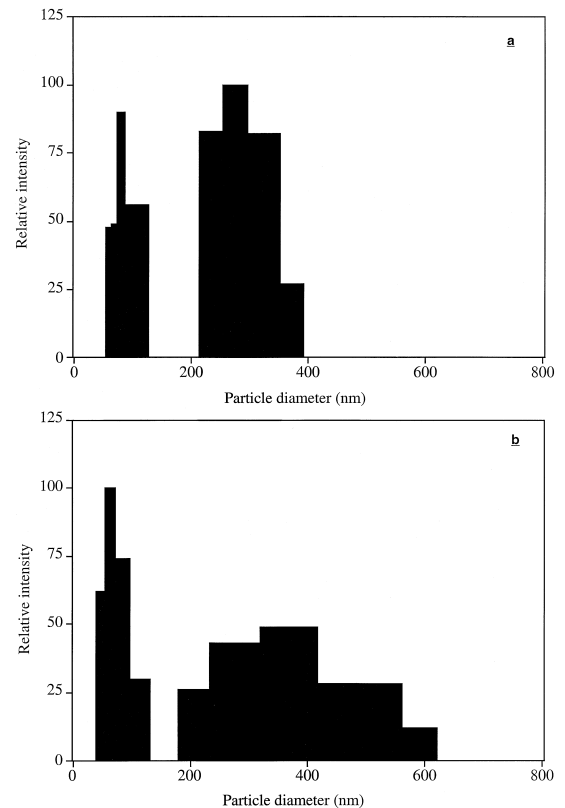


Fig. 6. Relative size distributions from the inner LSZ (a: average representation for stations 3–7) and the outer LSZ (b: average representation for stations 1–2) in June 1997 deduced from PCS. A bimodal size distribution was apparent with one of the maxima at 40–120 nm throughout the transect, whereas the larger maximum was limited to 200–400 nm in the inner LSZ while extending to above 600 nm at the outermost stations.

suspension at higher salinities but that matter indeed has aggregated into larger entities.

### 3.3. $^{238}\text{U}$ – $^{234}\text{Th}$ gauged scavenging intensity

#### 3.3.1. $^{234}\text{Th}$ method assumptions and considerations

Since the realization by Bhat et al. (1969) that the intensity of marine particle scavenging leaves an imprint on the  $^{238}\text{U}$ – $^{234}\text{Th}$  activity balance, the  $^{234}\text{Th}$  method has developed into a major tool for quantifying diverse particle processes, including colloid aggregation rates (e.g., Moran and Buesseler, 1993), and particle-mediated export of both bulk carbon (e.g., Coale and Bruland, 1985; Buesseler et

al., 1992a) and specific organic compounds (Gustafsson et al., 1997a). The method has been recently reviewed in detail elsewhere (Buesseler, 1998). In the simplest sense, the radiogenic deficit of highly particle-reactive  $^{234}\text{Th}$  ( $t_{1/2} = 24$  days) relative to its source, the highly soluble  $^{238}\text{U}$  ( $t_{1/2} = 4.5$  Byr), may be used as a measure of the intensity of particle-mediated export from surface regimes.

In principle, the  $^{234}\text{Th}$  method should reveal any significant particle removal during estuarine mixing giving rise to non-conservative distribution patterns as this tetravalent cation is well known to complex strongly both with oxide, carbonate, and other surface ligands common to natural waters. However, to realize this potential pay-off, there are several challenges that must be considered. First, the LSZ constitutes an environment with very low activity of the  $^{234}\text{Th}$  source  $^{238}\text{U}$  (e.g., the Kalix LSZ; Andersson et al., 1998, 2000). Second, a high presence of terrigenous HS may present sampling difficulties as humic-associated Th may be hard to collect. And finally, horizontal effects may significantly perturb the local  $^{238}\text{U} - ^{234}\text{Th}$  disequilibrium (Gustafsson et al., 1998). We did experience poor collection efficiencies with our  $\text{MnO}_2$ -impregnated adsorbers in this regime (0.12–0.46; Roos et al., in prep.) with the lowest values at the innermost stations, presumably because negatively-charged humic carriers of  $^{234}\text{Th}$  were repelled by the adsorber ( $\gamma\text{-MnO}_2$  has a point of zero charge,  $\text{pH}_{\text{zpc}} = 6$ , resulting in a net negative oxide surface at the local pH of around 7.5). However, in addition to our filtration train, large-volume precipitation of unfiltered total samples was also performed. The effect of horizontal transport on the local  $^{238}\text{U} - ^{234}\text{Th}$  disequilibrium has been found to be insignificant in regimes less quiescent than the extended Kalix LSZ (advective velocities around  $3 \text{ cm s}^{-1}$ ), and can thus be anticipated to not importantly influence the observed activities (Gustafsson et al., 1998; see also below).

### 3.3.2. $^{238}\text{U} - ^{234}\text{Th}$ -derived scavenging fluxes

The activity ratio between total  $^{234}\text{Th}$  and  $^{238}\text{U}$  throughout the LSZ region is suggestive of minimal settling removal. The  $^{238}\text{U}$  levels were explicitly measured in this study (Andersson et al., 2000). Uranium was found to behave conservatively with salinity along the LSZ transect. Total  $^{234}\text{Th}$  activities

were 0.1–0.3 dpm/l, resulting in a mean  $^{234}\text{Th}/^{238}\text{U}$  activity ratio of  $0.9 \pm 0.3$  (range 0.51–1.37) at the six LSZ stations (Fig. 7). These overall small deficits in a regime with such high colloid and particle concentrations may be contrasted to much smaller ratios of 0.05–0.3 common to other coastal regimes despite much lower suspended loads (e.g., Baskaran et al., 1992; Moran and Buesseler, 1993; Gustafsson et al., 1998). To further illustrate that, at least the studied LSZ is not a region of high-settling export, the  $^{234}\text{Th}$ -derived POC export fluxes for Kalix LSZ as a function of TOC was compared with estimates of the same flux from another well-studied continental shelf regime, the Gulf of Maine (Fig. 8). The Gulf of Maine data illustrate the dependency of OC export on suspended carbon concentrations typically found in most marine regimes (Buesseler, 1998). Despite several-fold higher TOC values in the Kalix LSZ, the  $^{234}\text{Th}$ -derived OC export estimates were much lower than in the Gulf of Maine ( $0\text{--}6 \text{ mmol m}^{-2} \text{ day}^{-1}$  in Kalix compared to an average of  $30 \text{ mmol m}^{-2} \text{ day}^{-1}$  in the Gulf of Maine). Hence, contrary to what one might have expected from previous studies of estuarine LSZ mixing, the U–Th data strongly suggest that there were no significant settling removal fluxes in the salinity 0.6–3 zone.

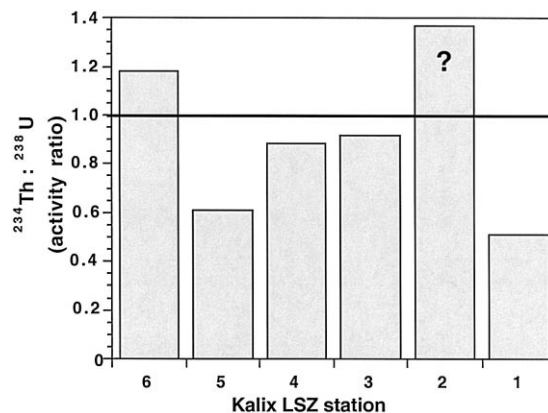


Fig. 7. Activity ratio (dpm/l) of  $^{234}\text{Th}/^{238}\text{U}$  throughout the Kalix LSZ. Despite high suspended matter loads (e.g., TOC ranged from 300 to  $500 \mu\text{M}$ ), large ratios were observed in this region. The  $> 1$  ratio at the innermost station 6 may plausibly reflect springflood resuspension of river-bed sediments, having become enriched in  $^{234}\text{Th}$  during the winter (it may also be a result of the very poor recovery of 27% at this station). The reason for the apparent  $> 1$  activity ratio at station 2 is unknown.

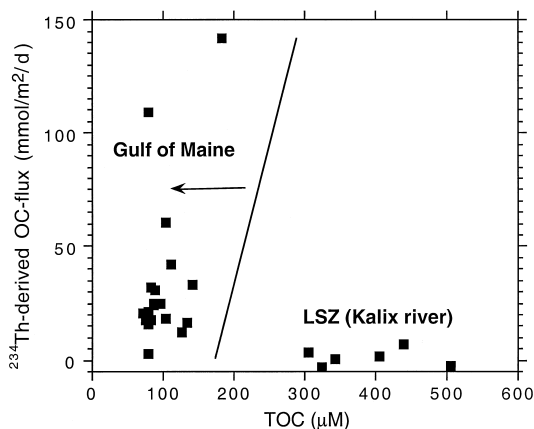


Fig. 8. The vertical export flux of POC from the mixed surface waters in the Kalix LSZ as a function of TOC was contrasted to the behavior in the Gulf of Maine (Gustafsson et al., unpub. data). This comparison illustrates both how little vertical export was actually taking place in the Kalix LSZ and its deviation from the commonly expected relationship between carbon export and TOC (e.g., Buesseler, 1998).

### 3.3.3. Size distribution and coagulation of $^{234}\text{Th}$

The size-fractionated  $^{234}\text{Th}$  distribution was also consistent with the aggregation-without-significant-settling scenario suggested by the other data. In particular, the fraction of total  $^{234}\text{Th}$  residing in the larger particulate ( $> 0.2 \mu\text{m}$ ) isolate was nearly 80% at the outermost LSZ station (station 1; salinity 3.03), while remaining between 24–33% at shoreward stations (Fig. 9). These detailed field results of mixing in the low-salinity range may indicate that significant coagulation of colloids to settling gravitoids may commence first around salinity 3. Given the high TOC and the low collection efficiencies of  $< 0.2 \mu\text{m}$   $^{234}\text{Th}$  on oxide adsorbents, it is likely that  $^{234}\text{Th}$  resides predominantly with the large colloidal pool within the LSZ, which — as espoused above — appears not to settle to any significant extent.

Due to its high particle-reactivity, it has been proposed that  $^{234}\text{Th}$  may be used as a “colloid coagulometer” (Honeyman and Santschi, 1989) to quantify the rate of matter aggregation or, inversely, the characteristic time that material is residing within a given size bin. We did attempt large-volume CFF for colloidal  $^{234}\text{Th}$  at two locations but were limited by losses to the CFF equipment. However, the isolated colloidal  $^{234}\text{Th}$  does represent a minimum ac-

tivity, and assigning either none or all of the lost  $^{234}\text{Th}$  exclusively to the colloidal pool allows the calculation of minimum and maximum possible colloidal residence times. For station 4 in the middle of the LSZ, a coagulometer calculation predicts that colloidal material in the 3 kD–0.2  $\mu\text{m}$  size bin (0.031–0.11 dpm/l) was aggregating at such a slow pace that the characteristic transfer time to achieve the  $> 0.2\text{-}\mu\text{m}$  size was on the order of 50–200 days. This may be contrasted to similarly estimated colloid residence times with respect to coagulation in the coastal regime of Buzzard’s Bay, MA, USA, of around 1 day (10 kD–0.2  $\mu\text{m}$ ; Moran and Buesseler, 1993) and 10 days in the offshore Sargasso Sea (10 kD–0.2  $\mu\text{m}$ ; Moran and Buesseler, 1992). Apparently, electrostatic repulsion effectively prevents humic colloids from coagulating to form aggregates  $> 0.2 \mu\text{m}$  at salinities  $< 3$  in real field settings such as the Kalix LSZ.

### 3.4. Modeling chemical transport in the LSZ

Given the uncertainty in addressing estuarine scavenging from property–salinity plots over narrow salinity ranges alone, a two-dimensional, two-box model was constructed to evaluate the relative importance of different transport vectors in the low salinity mixing zone.

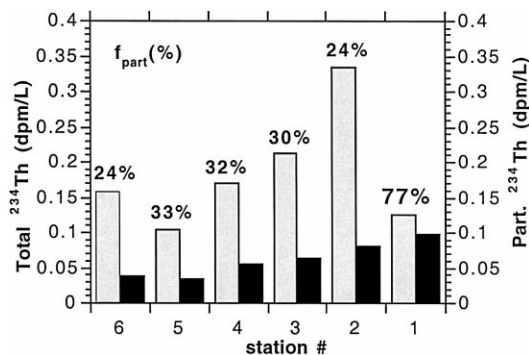


Fig. 9. The relative activities of total (leftmost lighter bars) and particulate  $^{234}\text{Th}$  (rightmost darker bars) in the Kalix LSZ. The analytical uncertainties were in the range of 1.5–5.2%. A larger fraction of  $^{234}\text{Th}$  in the particulate fraction (percentages listed above the bars) at the outermost station is consistent with its larger Th–U disequilibria (Fig. 7) and hypothesized aggregation at higher salinities.

3.4.1. Model dimension and parameterization

Consider that estuarine transport in the mixed surface layer of the Kalix River LSZ can be described by a two-dimensional two-box model. We assume that horizontal transport during the snowmelt runoff period is prevailing in a S–SW direction (Fig. 1). Thus, the model holds that onshore–offshore exchange is much more significant than across any alongshore gradients. Additionally, particle-mediated export vertically is explicitly included. The model construction is largely based on Gustafsson et al. (1998). We divided the Kalix LSZ into an inner box — topographically constrained by surrounding islands — and an offshore outer box, designated  $LSZ_i$  and  $LSZ_o$ , respectively (Figs. 1 and 10; Eqs. (1) and (2)). The detailed model dimensions and parameterization of advective and dispersive horizontal as well as settling-mediated vertical transport are summarized in Table 3. In addition to the low “strength” of the vertical scavenging mode revealed above, it was apparent that the calm conditions during and preceding our cruise resulted also in a slow net advection for the region. It is worth noting that spatially averaged settling rate coefficients derived independently with the  $^{234}\text{Th}$  method and sediment traps agreed within a factor of three in the inner LSZ and within 50% in the outer regime (Table 3).

Given the horizontal and vertical transport parameters, two-dimensional box models for any constituent of concentration  $C$  may be formulated for the surface layers of the Inner and Outer LSZ of the Kalix River estuary — for Inner LSZ:

$$\begin{aligned} \frac{\partial C_{LSZ_i}}{\partial t} = & + \frac{u_{r/i}}{x_i} C_r - \frac{(K_x)_{r/i}}{l_{r/i}} \frac{(C_{LSZ_i} - C_r)}{x_i} \\ & - \frac{u_{i/o}}{x_i} C_{LSZ_i} + \frac{(K_x)_{i/o}}{l_{i/o}} \frac{(C_{LSZ_o} - C_{LSZ_i})}{x_i} \\ & - k_{\text{settle}-i} C_{LSZ_{i,\text{part}}} \end{aligned} \quad (1)$$

for Outer LSZ:

$$\begin{aligned} \frac{\partial C_{LSZ_o}}{\partial t} = & + \frac{u_{i/o}}{x_o} C_{LSZ_o} - \frac{(K_x)_{i/o}}{l_{i/o}} \frac{(C_{LSZ_o} - C_{LSZ_i})}{x_o} \\ & - \frac{u_{o/f}}{x_o} C_{LSZ_o} + \frac{(K_x)_{o/f}}{l_{o/f}} \frac{(C_f - C_{LSZ_o})}{x_o} \\ & - k_{\text{settle}-o} C_{LSZ_{o,\text{part}}} \end{aligned} \quad (2)$$

where subscripts “r”, “i”, “o”, and “f” represent river, inner LSZ, outer LSZ, and off outer LSZ,

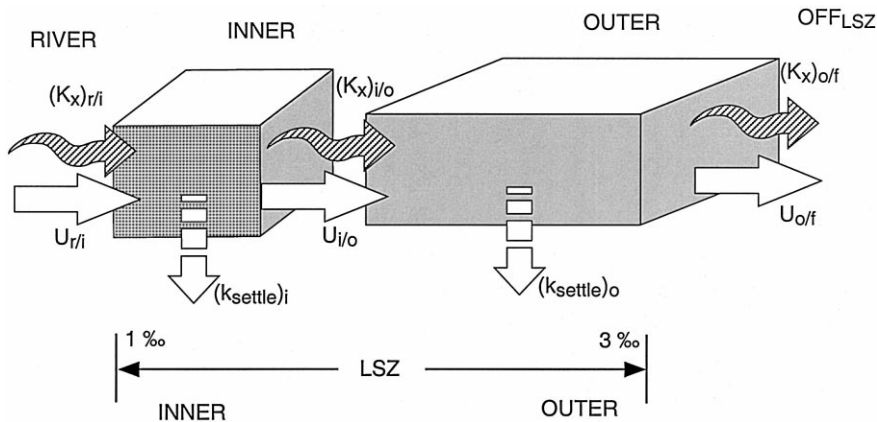


Fig. 10. Cartoon of a two-dimensional, two-box model of chemical mixing and transport through the Kalix River LSZ. The river end-member was represented by the lower river station Kamlunge,  $LSZ_{\text{inner}}$  comprised of stations 4, 5 and 6,  $LSZ_{\text{outer}}$  comprised of stations 2 and 3, and the offshore (Bothnic Bay) end-member was represented by  $Of_{LSZ}$  station 1. For areal delimitations, see Fig. 1, and for model parameterization and explanations of abbreviations, see Table 3.

Table 3  
Model parameters for the two-dimensional, two-box model of the LSZ off Kalix River

Parameter	Inner Kalix LSZ (LSZ <sub>i</sub> )	Outer Kalix LSZ (LSZ <sub>o</sub> )
<i>Transport length scales</i>		
Vertical		
Mixed layer depth; <sup>a</sup> shoreward boundary	$z_{r/i} = 8 \text{ m}$	$z_{i/o} = 6 \text{ m}$
Mixed layer depth; seaward boundary	$z_{i/o} = 6 \text{ m}$	$z_{o/f} = 6 \text{ m}$
Horizontal — advective		
Offshore box distance <sup>b</sup>	$x_i = 11 \text{ km}$	$x_o = 40 \text{ km}$
Horizontal — dispersive		
Characteristic gradient length scale, <sup>c</sup> shoreward	$l_{r/i} = 10 \text{ km}$	$l_{i/o} = 26 \text{ km}$
Characteristic gradient length scale, seaward	$l_{i/o} = 26 \text{ km}$	$l_{o/f} = 29 \text{ km}$
<i>Transport vectors</i>		
Net offshore advection <sup>d</sup>		
Shoreward boundary	$u_{r/i} = 0.02 \text{ m/s}$	$u_{i/o} = 0.03 \text{ m/s}$
Seaward boundary	$u_{i/o} = 0.03 \text{ m/s}$	$u_{o/f} = 0.03 \text{ m/s}$
Horizontal dispersion <sup>e</sup>		
Shoreward boundary	$(K_x)_{r/i} = 8.2 \text{ m}^2/\text{s}$	$(K_x)_{i/o} = 25 \text{ m}^2/\text{s}$
Seaward boundary	$(K_x)_{i/o} = 25 \text{ m}^2/\text{s}$	$(K_x)_{o/f} = 28 \text{ m}^2/\text{s}$
Vertical scavenging <sup>f</sup>		
<sup>234</sup> Th-derived apparent settling rate coefficient	$(k_{\text{settle}})_i = 0.034$	$(k_{\text{settle}})_o = 0.022 \text{ day}^{-1}$
Sediment-trap based apparent settling rate coefficient	$(k_{\text{settle}})_i = 0.105$	$(k_{\text{settle}})_o = 0.027 \text{ day}^{-1}$
<i>Box-weighted major element concentrations<sup>g</sup></i>		
Iron		
Total	4.8 $\mu\text{M}$	1.3 $\mu\text{M}$
Large particulate (> 0.2 $\mu\text{m}$ )	0.29 $\mu\text{M}$	0.095 $\mu\text{M}$
Silica		
Total	60 $\mu\text{M}$	39 $\mu\text{M}$
Large particulate (> 0.2 $\mu\text{m}$ )	0.50 $\mu\text{M}$	0.28 $\mu\text{M}$
Organic carbon		
TOC	426 $\mu\text{M}$	332 $\mu\text{M}$
POC	24 $\mu\text{M}$	19 $\mu\text{M}$

<sup>a</sup>Obtained from ocular inspection of two nearest CTD profiles.

<sup>b</sup>Length of each box in the offshore direction. The boundaries were selected based on hydrogeographical features (Fig. 1). The boundary between LSZ<sub>i</sub> and the river was taken as a straight line between Kusen and the southern tip of Halsö; between LSZ<sub>i</sub> and LSZ<sub>o</sub> stretches from Österbotten and a point half-way between southmost Halsö and Malören; the outer border of LSZ<sub>o</sub> as a line between Rödkallen and a point at the longitude of Malören and the latitude of Farstugrunden.

<sup>c</sup>The characteristic dispersive path lengths were taken as the distance from the mid-point of each box and either the mouth of the river (half-way between Läsno and Repskär), in between boxes, or off LSZ<sub>o</sub> to the known reference point station 1.

<sup>d</sup>Calculated estimates encompass the total contribution of both the cyclonic thermohaline circulation in the northern Bothnic Sea (Kullenberg, 1981; SMHI, 1986, 1993) and wind-induced advection (SMHI, 1993); the winds were merely 0–2 m/s with a N–NE direction preceding and during our expedition, in addition to the additional offshoreward advective component resulting from the Kalix River runoff during the height of springflood (Ingri, 1996).

<sup>e</sup>Horizontal dispersion coefficients were estimated from Okubo's diffusion diagrams (Okubo, 1971), with the above listed dispersive gradient length scales for the modeled sites. These numbers may be considered an upper limit as  $K_x$  in the northern Baltic appears generally recognized to be less than this standard method would predict (Kullenberg, 1981; SMHI, 1993).

<sup>f</sup>The apparent settling rate coefficients shown here, derived with two independent methods, reflect the mean for each box. Using the above <sup>238</sup>U and <sup>234</sup>Th data,  $k_{\text{settle}}$  was obtained according to the method in Gustafsson et al. (1997b). Fluxes of TSM into sediment traps positioned right below the pycnocline at stations 2, 4, and 6 were combined with mixed layer TSM inventories to derive  $k_{\text{settle}}$  estimates for traps.

<sup>g</sup>The concentrations of different constituents in each box has to be represented by a single value. Weighing factors were assigned based on the portion of offshoreward distance in each box that a station was closest to and thus supposedly best represented by. The river end-member concentration was taken as the Kamlunga (station 7) sample collected 16 June, and station 1 was used in determining the corresponding offshoreward concentration gradient for LSZ<sub>o</sub>.

respectively; and concentrations  $C$  with “part” in the subscript refer to particulate ( $> 0.2 \mu\text{m}$ ) concentrations and all other  $C$  are representing total unfil-tered concentrations for each box.

### 3.4.2. Model predictions

The model output suggested that horizontal advection was dominating over both dispersion and vertical scavenging as the major transport mode for Fe, Si, and organic carbon in the LSZ. Of potential relevance for the OC results, the model assumes no internal sinks (e.g., remineralization) or sources (e.g., primary production). The absence of any significant marine biosynthesis was in addition to measured low primary production rates supported by the very terrestrial signature of the  $\delta^{13}\text{C}$  throughout the entire transect (Table 1).

Horizontal advection appears to dominate the transport fate of OC in both the inner and outer LSZ (Table 4). The model results suggest that, at most, 5% of the OC may be exported vertically. This result is consistent with the apparently linear and conservative mixing trends for TOC and HS field data presented above. This is further consistent with the particle composition and size distribution arguments presented above as well as with the small  $^{238}\text{U}$ – $^{234}\text{Th}$  disequilibria, indicating minimal particle removal.

The minor fraction of TOC that still may be lost could be a portion of the humic acid fraction, which does appear to drop off faster than TOC with distance (although this may also be due to the potentially dynamic nature of its fluorescence quantum yield, as discussed above).

Similarly, horizontal advection appears to be the largest transport vector for iron in the LSZ (Table 4 and Fig. 11). Also, for Fe, about 5% of what entered the LSZ from the river was removed downward. About equal magnitudes were being removed in the inner and outer domains of the LSZ. Non-conservativeness of the order found here for OC and Fe is not unlikely to pass unnoticed in evaluation of property–salinity plots over limited (LSZ) salinity ranges for dynamic regimes and thus impress the usefulness of complementary two-dimensional estuarine LSZ modeling facilitated by simultaneous collection of  $^{234}\text{Th}$  data. Their small but similar removal efficiencies may suggest that Fe and OC are part of the same gravitoid forms (Gustafsson and Gschwend, 1997), which very well may be dominated by humic-coated iron oxyhydroxides. In contrast, for silica,  $< 1\%$  was indicated to be exported vertically (Table 4). This mixing conservativeness for Si was consistent with what has been found in many other estuaries (e.g., Boyle et al., 1974).

Table 4

Results of two-dimensional, two-box<sup>a</sup> modeling of chemical transport through the Kalix LSZ

Location/transport mode	OC ( $\mu\text{M day}^{-1}$ )	Fe ( $\mu\text{M day}^{-1}$ )	Si ( $\mu\text{M day}^{-1}$ )	Conductivity ( $\text{mS cm}^{-1} \text{day}^{-1}$ )
<b>Inner LSZ</b>				
Advection from river	+79	+1.2	+10.0	+0.17
Dispersion from river	+0.5	+0.02	+0.014	−0.22
Advection to outer LSZ	−100	−1.1	−15	−8.4
Dispersion to outer LSZ	−0.7	−0.03	−0.16	+0.15
Settling/inner LSZ: $^{234}\text{Th}$	−2.5	−0.03	−0.05	0
Traps	−0.8	−0.01	−0.02	0
<b>Outer LSZ</b>				
Advection from inner LSZ	+28	+0.31	+4.0	+2.32
Dispersion from inner LSZ	+0.2	+0.007	+0.046	−0.041
Advection to off LSZ	−22	−0.086	−2.6	−3.6
Dispersion to off LSZ	−0.01	−0.002	−0.011	+0.008
Settling/outer LSZ: $^{234}\text{Th}$	−0.5	−0.0025	−0.007	0
Traps	−0.4	−0.0022	−0.007	0

<sup>a</sup>The smaller dimension of Inner LSZ relative to Outer LSZ (factor of 0.32) needs to be taken into account when evaluating the total mass fluxes through the LSZ.

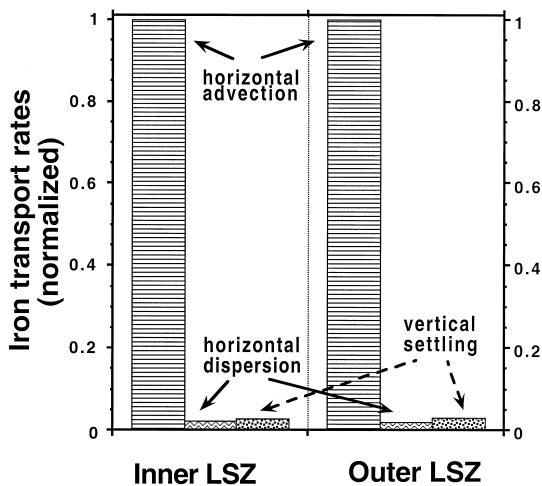


Fig. 11. Comparison of the relative importance of horizontal (advective and dispersive) and vertical (particle-mediated settling) transport of iron in the Inner and Outer LSZ. The three different transport modes are normalized to the dominant loss route in each box (horizontal advection).

The total export (horizontal plus vertical) of these elements from the LSZ were at the time of our observations less than the riverine input. While the model suggested that export of OC and Si constituted 80–90% of the import, this number was only 25% for Fe. The hydraulic stage of the system was evaluated through applying the model to conductivity as a definite conservative tracer. Advection was found to dominate both the inner and outer LSZ. The system was clearly in a non-steady state. However, offshoreward advection overwhelmed onshore dispersion (Table 4). The snowmelt runoff was leading to a push of the isohalines outward, and thus negative (decreasing) salinities in the Eulerian dimension must have existed. Most likely, the first half (building stage) of the spring flood was currently propagating through the estuary. This is consistent with temporal data from our upstream river monitoring station Kamlunge (Ingri et al., 2000) and a travel time from advection estimates of a few weeks for the 70 km distance. The greater imbalance for Fe plausibly results from its larger river–ocean concentration gradient, making its LSZ mass balance more sensitive to non-steady state mixing stages. The small deficits for both OC and Si suggests that the spring runoff must have been close to reaching its seasonal peak.

#### 4. Concluding discussion

A broad spectrum of biogeochemical parameters suggest that both iron oxyhydroxides and organic matter were aggregating but not significantly settling during transport through the quiescent 60 km long low salinity mixing zone (up to salinity 3) of the Kalix River–Bothnic Bay. Minimal removal of Fe, Si, and OC was suggested by (a) apparently linear property–salinity plots from 3 different years, (b) parallel laboratory mixing experiments, (c) small  $^{238}\text{U}$ – $^{234}\text{Th}$  disequilibria throughout the LSZ transect, and (d) by the result of an independent two-dimensional two-box model of LSZ transport.

During advective offshore transport, there were strong indications of significant aggregation taking place along the LSZ transect. Ultrafiltered size-distributions of OC revealed a shift from dissolved to colloidal and larger particulate forms as the salinity increased, despite decreasing overall organic matter loads. An apparently decreasing fluorescence quantum yield of HS along the transect is suggestive of increased packaging of at least the chromophoric moieties into larger and “tighter” aggregates. It is worth noting that measurements of primary production rates and  $\delta^{13}\text{C}$  of POC support a constant source (terrestrially dominated) of the organic matter, thus, suggesting a dominance of an abiotic aggregation process. In a further support of the transectual aggregation-without-sedimentation scenario, light scattering techniques (PCS) were implying that the distribution of the suspended matter was skewed to larger sizes at higher salinities.

While aggregation processes becoming induced at higher salinities certainly was no surprise, the lack of removal of Fe and OC in the quiescent estuarine LSZ is counter to expectations from earlier mixing studies. We believe the poor particulate removal efficiency in the Kalix estuary LSZ resulted from the high organic-matter-to-detrital mineral load in this system. A determinant variable for settling velocity is the wet density difference between the particulate aggregate and the surrounding seawater medium ( $\rho_{\text{agg}} - \rho_{\text{sw}}$ ). Highly amorphous and loosely-structured, pure organic aggregates could be expected to have wet densities insignificantly different from that of the surface water (1.00–1.04 g cm<sup>-3</sup>), whereas detrital particles or authigenic inorganic tests may

have densities in the range of 2.5–3 g cm<sup>-3</sup>. Hence, even small variations in how much minerals are associated with an aggregate may have a large effect on its net buoyancy. This has recently been demonstrated to affect the relative fluxes of particulate organic and inorganic carbon in the equatorial Pacific region (Hernes et al., 2000). The Kaix River — like its neighboring and geochemically similar Russian Arctic “black” rivers — has a relatively high organic carbon load. The TOC/TSM mass ratio during Kalix springflood is about 0.50 (Ingri, 1996), whereas this value is ≤ 0.10 in “average world river” (Ittekkott and Laane, 1991).

The growing evidence for the important role of detrital and minerogenic “sinks” on vertical aggregate fluxes in marine systems calls for a functional approach to separation of different carrier phases. As with the thermodynamic distinction between dissolved and colloidal entities, it is clear that a separation of hydrodynamically distinct colloids and gravitoids cannot be performed by size-based filtration (Gustafsson and Gschwend, 1997). In this respect, particle separation techniques based on “hydrodynamic chromatography” such as SPLITT (Giddings, 1988) appear particularly promising. The aggregation-without-settling behavior for detrital-poor rivers such as the Kalix and its neighboring but northward-flowing Russian Arctic rivers may have as one implication a smaller trapping in the vicinity of the river mouth and instead a potential for off-shelf transport of a larger than expected fraction of the river-borne matter.

### Acknowledgements

For assistance during sampling and analysis, we gratefully acknowledge Henning Holmström, Magnus Land, Brian Schoeman, and Molly Zacher (and California Institute of Technology SURF program for supporting her participation in the project), as well as the crew and captain of R/V KBV005 of the UMF Umeå Marine Research Center. This project has been carried out with financial support from the Swedish Natural Science Research Council in the form of research grant NFR # G-AA/GU 08483-310 (to JI et al.), NFR # G-GU 6331-317 (to PA et al.) and NFR # 1-AA/GB 12291-301 (to ÖG et al.). Additionally, ÖG was supported by a post-doctoral

fellowship from the Swedish Natural Science Research Council (NFR # G-GU 6331-316).

### References

- Andersson, P.S., Wasserburg, G.J., Chen, J.H., Papanastassiou, D.A., Ingri, J., 1995. <sup>238</sup>U–<sup>234</sup>U and <sup>232</sup>Th–<sup>230</sup>Th in the Baltic Sea and in river water. *Earth Planet. Sci. Lett.* 130, 217–234.
- Andersson, P.S., Porcelli, D., Wasserburg, G.J., Ingri, J., 1998. Particle transport of <sup>234</sup>U–<sup>238</sup>U in the Kalix River and in the Baltic Sea. *Geochim. Cosmochim. Acta* 62, 385–392.
- Andersson, P.S., Porcelli, D., Gustafsson, Ö., Ingri, J., Wasserburg, G.J., 2000. The importance of colloidal particles for the behavior of uranium isotopes in the low salinity zone of a stable estuary. *Geochimica Cosmochimica Acta*, (in press).
- Baskaran, M., Santschi, P.H., Benoit, G., Honeyman, B.D., 1992. Scavenging of thorium isotopes by colloids in seawater of the Gulf of Mexico. *Geochim. Cosmochim. Acta* 56, 3375–3388.
- Berne, B., Pecora, R., 1976. *Dynamic Light Scattering with Applications to Chemistry, Biology and Physics*. Wiley-Interscience, New York.
- Bhat, S.G., Krishnaswami, S., Lal, D., Rama, Moore, W.S., 1969. <sup>234</sup>Th/<sup>238</sup>U ratios in the ocean. *Earth Planet. Sci. Lett.* 5, 483–491.
- Boström, K., Wiborg, L., Ingri, J., 1982. Geochemistry and origin of ferromanganese concretions in the Gulf of Bothnia. *Mar. Geol.* 50, 1–24.
- Boyle, E.A., Collier, R., Dengler, A.T., Edmond, J.M., Ng, A.C., Stallard, R.F., 1974. On the chemical mass-balance in estuaries. *Geochim. Cosmochim. Acta* 38, 1719–1728.
- Boyle, E.A., Edmond, J.M., Sholkovitz, E.R., 1977. The mechanism of iron removal in estuaries. *Geochim. Cosmochim. Acta* 41, 1313–1324.
- Buesseler, K.O., Bacon, M.P., Cochran, J.K., Livingston, H.D., 1992a. Carbon and nitrogen export during the JGOFS North Atlantic Bloom Experiment estimated from <sup>234</sup>Th:<sup>238</sup>U disequilibria. *Deep-Sea Res.* 39, 1115–1137.
- Buesseler, K.O., Cochran, J.K., Bacon, M.P., Livingston, H.D., Casso, S.A., Hirschberg, D., Hartman, M.C., Fleer, A.P., 1992b. Determination of thorium isotopes in seawater by non-destructive and radiochemical procedures. *Deep-Sea Res.* 39, 1103–1114.
- Buesseler, K.O., Bauer, J., Chen, R., Eglinton, T., Gustafsson, Ö., Landing, W., Mopper, K., Moran, S.B., Santschi, P., VernonClark, R., Wells, M., 1996. *Mar. Chem.* 55, 1–31.
- Buesseler, K.O., 1998. The decoupling of production and particulate export in the surface ocean. *Global Biogeochem. Cycles* 12, 297–310.
- Burman, J.-O., Pontér, C., Boström, K., 1978. Metaborate digestion procedure for inductively coupled plasma-optical emission spectrometry. *Anal. Chem.* 50, 679–680.
- Carroll, J., Moore, W.S., 1994. Uranium removal during low discharge in the Ganges–Brahmaputra mixing zone. *Geochim. Cosmochim. Acta* 58, 4987–4995.
- Chen, J.H., Edwards, R.L., Wasserburg, G.J., 1986. <sup>238</sup>U, <sup>234</sup>U and <sup>232</sup>Th in seawater. *Earth Planet. Sci. Lett.* 80, 241–251.

- Chu, B., 1974. Laser Light Scattering. Academic Press, New York.
- Coale, K.H., Bruland, K.W., 1985.  $^{234}\text{Th}$ – $^{238}\text{U}$  disequilibria within the California. *Curr. Limnol. Oceanogr.* 30, 22–33.
- Dai, M.H., Martin, J.M., 1995. First data on the trace metal level and behavior in two major Arctic river-estuarine systems (Ob and Yenisey) and in the adjacent Kara Sea, Russia. *Earth Planet. Sci. Lett.* 131, 127–141.
- Dai, M.H., Buesseler, K.O., Ripple, P., Andrews, J., Belastock, R.A., Gustafsson, Ö., Moran, S.B., 1998. Evaluation of two cross-flow ultrafiltration membranes for isolating marine organic colloids. *Mar. Chem.* 62, 117–136.
- Elderfield, H., Upstill-Goddard, R., Sholkovitz, E.R., 1990. The rare earth elements in rivers, estuaries and coastal seas and their significance to the composition of ocean waters. *Geochim. Cosmochim. Acta* 54, 971–991.
- Elmgren, R., 1984. Trophic dynamics in the enclosed, brackish Baltic Sea. *Rap. P.-v. Reun. Cons. Int. Explor. Mer.* 183, 152–163.
- Farley, K.J., Morel, F.M.M., 1986. Role of coagulation in the kinetics of sedimentation. *Environ. Sci. Technol.* 20, 187–195.
- Giddings, J.C., 1988. Continuous separation in split-flow thin (SPLITT) cells: potential applications to biological materials. *Sep. Sci. Technol.* 23, 931–943.
- Gustafsson, Ö., Buesseler, K.O., Gschwend, P.M., 1996. On the integrity of cross-flow filtration for collecting marine organic colloids. *Mar. Chem.* 55, 93–111.
- Gustafsson, Ö., Gschwend, P.M., Buesseler, K.O., 1997a. Using  $^{234}\text{Th}$  disequilibria to estimate the vertical removal rates of polycyclic aromatic hydrocarbons from the surface ocean. *Mar. Chem.* 57, 11–23.
- Gustafsson, Ö., Gschwend, P.M., Buesseler, K.O., 1997b. Settling removal rates of PCBs into the northwestern Atlantic derived from  $^{238}\text{U}$ – $^{234}\text{Th}$  disequilibria. *Environ. Sci. Technol.* 31, 3544–3550.
- Gustafsson, Ö., Gschwend, P.M., 1997. Aquatic colloids: concepts, definitions, and current challenges. *Limnol. Oceanogr.* 42, 519–528.
- Gustafsson, Ö., Buesseler, K.O., Geyer, W.R., Moran, S.B., Gschwend, P.M., 1998. An assessment of the relative importance of horizontal and vertical transport of particle-reactive chemicals in the coastal ocean. *Cont. Shelf Res.* 18, 805–829.
- Hartman, M.C., Buesseler, K.O., 1994. Woods Hole Oceanographic Institution Technical Report, WHOI-94-15. 16 pp.
- Heikkinen, K., 1994. Organic matter, iron and nutrient transport and nature of dissolved organic matter in the drainage basin of a boreal humic river in northern Finland. *Sci. Total Environ.* 152, 81–89.
- HELCOM, 1988. Guidelines for the Baltic monitoring programme for the third stage: part D. Biological determinands. *Balt. Sea Environ. Proc.* (27D).
- Hernes, P.J., Peterson, M.L., Murray, J.W., Wakeham, S.G., Lee, C., Hedges, J.I., 2000. Particulate carbon and nitrogen fluxes and compositions in the central equatorial Pacific. (submitted.)
- Honeyman, B.D., Santschi, P.H., 1989. A Brownian-pumping model for oceanic trace metal scavenging: evidence from Th isotopes. *J. Mar. Res.* 47, 951–992.
- Ingri, J., Pontér, C., 1986. Iron and manganese layering in recent sediments in the Gulf of Bothnia. *Chem. Geol.* 56, 105–116.
- Ingri, J., Widerlund, A., 1994. Uptake of alkali and alkaline-earth elements on suspended iron and manganese in the Kalix River, northern Sweden. *Geochim. Cosmochim. Acta* 58, 5433–5442.
- Ingri, J., 1996. Kalixälvens hydrogeokemi. Länsstyrelsen i Norrbotten rapportserie 2, 128 pp. (In Swedish).
- Ingri, J., Torssander, P., Andersson, P.S., Mörth, C.-M., Kusabe, M., 1997. Hydrogeochemistry of sulfur isotopes in the Kalix River catchment, northern Sweden. *Appl. Geochem.* 12, 483–496.
- Ingri, J., Widerlund, A., Land, M., Gustafsson, Ö., Andersson, P.S., Öhlander, B., 2000. Temporal variations in the fractionation of the rare earth elements in a boreal river; the role of colloidal particles. *Chem. Geol.* 166, 23–45.
- Ittekkott, V., Lane, R.W.P.M., 1991. Fate of riverine particulate organic matter. In: Degens, E.T., Kempe, S., Richey, J.E. (Eds.), *Biogeochemistry of Major World Rivers*. Wiley, pp. 233–243.
- Kalle, K., 1949. Fluoreszenz und Gelbstoff im Bottnischen und Finnischen Meerbusen. *Dtsch. Hydrogr. Z.* 2, 9–124. (In German).
- Karlsson, S., Petersson, A., Håkansson, K., Ledin, A., 1994. Fractionation of trace metals in surface water with screen filters. *Sci. Tot. Environ.* 149, 215–223.
- Kershaw, R.L., 1986. A new model for the humic materials and their interactions with hydrophobic organic chemicals in soil–water or sediment–water systems. *J. Contam. Hydrol.* 1, 29–45.
- Kraepiel, A.M.L., Chiffolleau, J.-F., Martin, J.-M., Morel, F.M.M., 1997. Geochemistry of trace metals in the Gironde estuary. *Geochim. Cosmochim. Acta* 61, 1421–1436.
- Kullenberg, G., 1981. Physical oceanography. In: Voipio, A. (Ed.), *The Baltic Sea*. Elsevier, Amsterdam, pp. 135–181.
- Larsson, U., Blomqvist, S., Abrahamsson, B., 1986. A new sediment trap system. *Mar. Ecol. Prog. Ser.* 31, 205–207.
- Lebo, M.E., Sharp, J.H., Cifuentes, L.A., 1994. Contribution of river phosphate variations to apparent reactivity estimated from phosphate–salinity diagrams. *Estuarine Coastal Shelf Sci.* 39, 583–594.
- Ledin, A., Karlsson, S., Düker, A., Allard, B., 1993. Applicability of photon correlation spectroscopy for measurement of concentration and size distribution of colloids in natural waters. *Anal. Chim. Acta* 281, 421–428.
- Loder, T.C., Reichard, R.P., 1981. The dynamics of conservative mixing in estuaries. *Estuaries* 4, 64–69.
- Moran, S.B., Buesseler, K.O., 1992. Short residence time of colloids in the upper ocean estimated from  $^{238}\text{U}$ – $^{234}\text{Th}$  disequilibria. *Nature* 359, 221–223.
- Moran, S.B., Buesseler, K.O., 1993. Size-fractionated  $^{234}\text{Th}$  in continental shelf waters off New England: implications for the role of colloids in oceanic trace metal scavenging. *J. Mar. Res.* 51, 893–922.
- Officer, C.B., 1979. Discussion of the behaviour of nonconservative dissolved constituents in estuaries. *Estuarine Coastal Mar. Sci.* 9, 91–94.
- Ödman, F., Ruth, T., Pontér, C., 1999. Validation of a field

- filtration technique for characterization of suspended particulate matter from seawater: Part I. Major elements. *Appl. Geochem.* 14, 301–317.
- Öhlander, B., Land, M., Ingri, J., Widerlund, A., 1996. Mobility of rare earth elements during weathering of till in northern Sweden. *Appl. Geochem.* 11, 93–99.
- Okubo, A., 1971. Oceanic diffusion diagrams. *Deep-Sea Res.* 18, 789–802.
- Perret, D., Newman, M.E., Nègre, J.-C., Chen, Y., Buffle, J., 1994. Submicron particles in the Rhine River — I. Physico-chemical characterization. *Water Resour.* 28, 91–106.
- Pettersson, C., Allard, B., Boren, H., 1997. River discharge of humic substances and humic-bound metals to the Gulf of Bothnia. *Estuarine Coastal Shelf Sci.* 44, 533–541.
- Pickard, G.L., Emery, W.J., 1990. *Descriptive Physical Oceanography*. 5th Pergamon, 320 pp.
- Pontér, C., Ingri, J., Burman, J.-O., Boström, K., 1990. Temporal variations in dissolved and suspended iron and manganese in the Kalix River, northern Sweden. *Chem. Geol.* 81, 121–131.
- Pontér, C., Ingri, J., Boström, K., 1992. Geochemistry of manganese in the Kalix River, northern Sweden. *Geochim. Cosmochim. Acta* 56, 1485–1494.
- Porcelli, D., Andersson, P.S., Wasserburg, G.J., Ingri, J., Baskaran, M., 1997. The importance of colloids and mires for the transport of uranium isotopes through the Kalix River watershed and the Baltic Sea. *Geochim. Cosmochim. Acta* 61, 4095–4113.
- Rodushkin, I., Ruth, T., 1997. Determination of trace metals in estuarine and sea-water reference materials by high resolution inductively coupled plasma mass spectrometry. *J. Anal. At. Spectrom.* 12, 1181–1185.
- Romankevich, E.A., 1984. *Geochemistry of Organic Matter in the Ocean*. Springer, Berlin.
- Schurtenberger, P., Newman, M., 1993. Characterization of biological and environmental particles using static and dynamic light scattering. In: Van Leeuwen, H.P., Buffle, J. (Eds.), *Environmental Particles II*. Lewis, Chelsea, MI.
- Shiller, A.M., Boyle, E.A., 1991. Trace elements in the Mississippi River delta outflow region: behavior at high discharge. *Geochim. Cosmochim. Acta* 55, 3241–3251.
- Sholkovitz, E., 1976. Flocculation of dissolved organic and inorganic matter during mixing of river water and seawater. *Geochim. Cosmochim. Acta* 40, 831–845.
- Sholkovitz, E., Boyle, E.A., Price, N.B., 1978. The removal of dissolved humic acids and iron during estuarine mixing. *Earth Planet. Sci. Lett.* 40, 130–136.
- Skoog, A., Wedborg, M., Fogelqvist, E., 1996. Photobleaching of fluorescence and the organic carbon concentration in a coastal environment. *Mar. Chem.* 55, 333–345.
- SMHI, 1986. Calculations of horizontal exchange coefficients using Eulerian time series current meter data from the Baltic Sea, Reports on Oceanography No. 1. Swedish Meteorological and Hydrological Institute, SMHI, Norrköping, Sweden.
- SMHI, 1993. The Gulf of Bothnia year 1991 physical transport experiments, Reports on Oceanography No. 15. Swedish Meteorological and Hydrological Institute, SMHI, Norrköping, Sweden.
- Thurman, E.M., 1985. *Organic Geochemistry of Natural Waters*. Martinus Nijhoff/W. Junk Publishers, Dordrecht, 497 pp.
- Turekian, K., 1977. The fate of metals in the ocean. *Geochim. Cosmochim. Acta* 41, 1139–1144.
- Wedborg, M., Skoog, A., Fogelqvist, E., 1994. Organic carbon and humic substances in the Baltic Sea, Kattegatt, and the Skagerrak. In: Senesi, N., Miano, T.M. (Eds.), *Humic Substances in the Global Environment*. Elsevier.
- Widerlund, A., 1996. Suspended particulate matter, sedimentation and early diagenetic processes in the Kalix River estuary, northern Sweden. PhD thesis, Luleå Univ. Technol.